metals

MDPI

Article

Springback Analysis of Flexible Stretch Bending of Multi-Point Roller Dies Process for Y-Profile under Different Process Parameters

Chuandong Chen [1,2], Jicai Liang [1,2], Yi Li [1], Ce Liang [1] and Wenming Jin [1,2,*]

[1] Key Laboratory of Automobile Materials, College of Materials Science and Engineering, Jilin University, Ministry of Education, Changchun 130025, China; chencd19@mails.jlu.edu.cn (C.C.); liangjicai@jlu.edu.cn (J.L.); henrylee@jlu.edu.cn (Y.L.); liangce@jlu.edu.cn (C.L.)
[2] Roll Forging Research Institute, Jilin University, Changchun 130025, China
* Correspondence: jwmjlu@126.com

Abstract: Springback is a common defect caused by elastic recovery in the plastic forming process, which can cause the formed workpiece to deviate from the target shape. The purpose of this paper is to grasp the influence law of process parameters on springback deviation so as to optimize process parameters to reduce springback. Taking the Y-profile as the research object, the influence of process parameters such as horizontal bending radius, vertical bending radius, transition zone length, radius of roller dies, and wall thickness of the profile on springback deviation is discussed by numerical simulation. Additionally, the validity of the numerical simulation is verified through experiments. The springback law obtained by numerical simulation is applied to practical production, and the large-scale production of the Y-profile is realized.

Keywords: stretch bending; multi-point bending; springback; process parameters; numerical modelling

Citation: Chen, C.; Liang, J.; Li, Y.; Liang, C.; Jin, W. Springback Analysis of Flexible Stretch Bending of Multi-Point Roller Dies Process for Y-Profile under Different Process Parameters. *Metals* **2021**, *11*, 646. https://doi.org/10.3390/met11040646

Academic Editors: Jean-Michel Bergheau and Ricardo J. Alves de Sousa

Received: 9 March 2021
Accepted: 13 April 2021
Published: 15 April 2021

1. Introduction

Springback is a phenomenon caused by elastic recovery after unloading. The radius of curvature of any bending fiber increases after the bending moment is removed. Springback has always been one of the main factors affecting the forming accuracy of parts in the plastic forming process. Due to the existence of springback, the geometric shape of a part does not fully conform to the target shape. Therefore, the shape accuracy of the parts cannot meet the design requirements [1–3].

In order to better describe the springback behavior during plastic forming, many scholars have conducted substantial research. Wu et al. established a new model to describe the springback behavior of space tubes, and extended the model [4] to different loading modes and hardening materials. The new model effectively described the springback behavior of space tubes [5]. Zhang et al. proposed a new 3D optical method to measure and evaluate springback in the forming process and studied its principles, procedures, and steps [6]. Ouakdi et al. used the U-shaped tensile-bending test to evaluate springback, showing the influence of factors such as the radius of curvature of die, the blank holding force (BHF), and the depth of drawing on springback [7]. Wasif et al. established the analysis model of springback prediction for the combination of blank thickness, width, bending angle, and machine parameters, and evaluated the optimal combination of minimum springback parameters [8]. In order to study the deformation and springback behavior of 3D tubes under complex stress conditions, Zhang et al. proposed a new semi-analytical method to predict springback behavior of 3D tubes [4]. When applying this method to predict the springback of a typical 3D tube, the comparison of theoretical and experimental results showed that the method had significant consistency.

Many scholars have studied and discussed the springback law in the plastic forming process. The bending springback model of the analytical elastic–plastic tube was established by Zhan et al. The changes of Young's modulus, wall thickness, and neutral layer were considered in this model [9]. Vasudevan studied the springback behavior of electro-galvanized sheets in the process of air bending [10]. Based on a springback test, Daxin et al. mastered the law of springback angle-changing with material parameters under certain pipe sizes and bending conditions [11,12]. Farhadi et al. considered the nonlinear kinematic hardening model when studying springback, and they analyzed the numerical solution of a springback problem on thick-walled pipe [13]. Ozturk et al. studied the springback behavior of hardened 5083-H111 aluminum magnesium alloy with a thickness of 3 mm at different temperatures [14]. Rahmani et al. used finite element and experimental methods to conduct V-bending, and they studied the effects of different parameters on the springback phenomenon [15].

It is helpful to reduce the springback deviation to master the springback law in the plastic forming process. Li et al. proposed a multi-step multi-point forming method to reduce the springback in the multi-point forming process [16]. Abebe et al. used the RBF prediction model to find the optimal value for reducing and compensating the springback induced by different blank thicknesses [17]. Wang et al. studied the springback under pure bending conditions, and they determined the effects of blank and die temperature, die gap, and die corner radius [18]. Liu et al. studied the springback behavior of 6063 aluminum curved profiles during the forming process and proposed the best process method for processing profiles [19].

Based on the idea of flexible forming, Liang et al. proposed a flexible stretch bending of multi-point roller dies (FSB-MPRD) forming technology, which realized the one-time forming of the 3D deformation of profile [20]. In order to grasp the law of springback in the FSB-MPRD process, the effect of process parameters such as horizontal bending radius, vertical bending radius, transition zone length, radius of roller dies, and wall thickness of profile on springback deviation was studied by using ABAQUS finite element software and verified by experiments. At present, the research on springback defects in the 2D stretch bending process is more extensive than the research on springback defects in the 3D stretch bending process. Mastering the influence of process parameters on springback defects in the 3D stretch bending process is helpful to better control springback defects.

2. Materials and Methods

2.1. Material Model

The material of the blank was 6082 aluminum alloy in the T6 heat treatment state. The shape and size of tensile parts were set according to GBT228-2002 tensile specimen standard. The WDW-300 universal tensile testing machine (Kason, Jinan, China) was used for uniaxial tensile test, and the tensile fracture parts are shown in Figure 1. The stress–strain curve of 6082 aluminum alloy was determined according to three sets of tensile tests, as shown in Figure 1. The main mechanical properties of 6082-T6 aluminum alloy are shown in Table 1. According to the von Mises yield criterion and plastic flow rule, the stress–strain relationship obeys the power hardening material model, as shown in Equation (1):

$$\sigma = \begin{cases} E\varepsilon, \varepsilon < \varepsilon_s \\ K\varepsilon^n, \varepsilon \geq \varepsilon_s \end{cases} \quad (1)$$

where σ is stress, ε is strain, E is Young's modulus, K is strength coefficient, n is hardening exponent, and ε_s is yield strain.

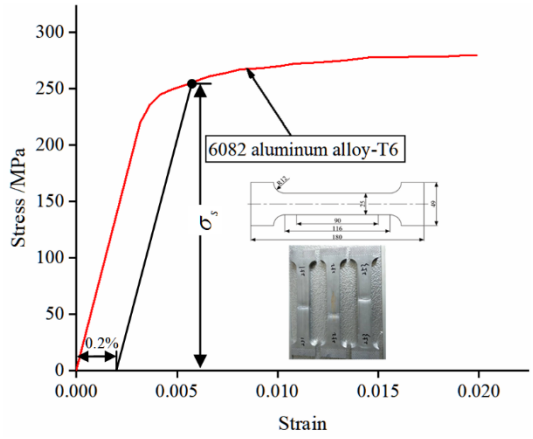

Figure 1. Stress–strain curve of 6082 aluminum alloy.

Table 1. Mechanical properties of aluminum alloy 6082-T6.

E/GPa	*V*	σ_s/MPa	ρ/g·cm^{-3}	*K*/MPa	*N*
70	0.33	254	2.71	418.7	0.105

2.2. Forming Method

Figure 2 shows the forming principle of the FSB-MPRD process. Figure 2a shows the horizontal bending process of the workpiece. Figure 2b shows the vertical bending process of the workpiece. The multi-point roller die (MPRD) was installed on the flexible foundation unit (FFU), the FFU was regularly arranged, and the surface was adjustable. In the 3D stretch bending process, the horizontal bending angle can be increased or decreased by changing the position of the FFU, and the vertical bending angle can be increased or decreased by changing the moving distance of the MPRD. By changing the shape of the MPRD, various workpieces with complex cross-sections can be formed. Therefore, this advanced processing technology can not only form 3D workpieces but can also save the manufacturing cost of die and greatly improve production efficiency and the mechanical properties of products [20].

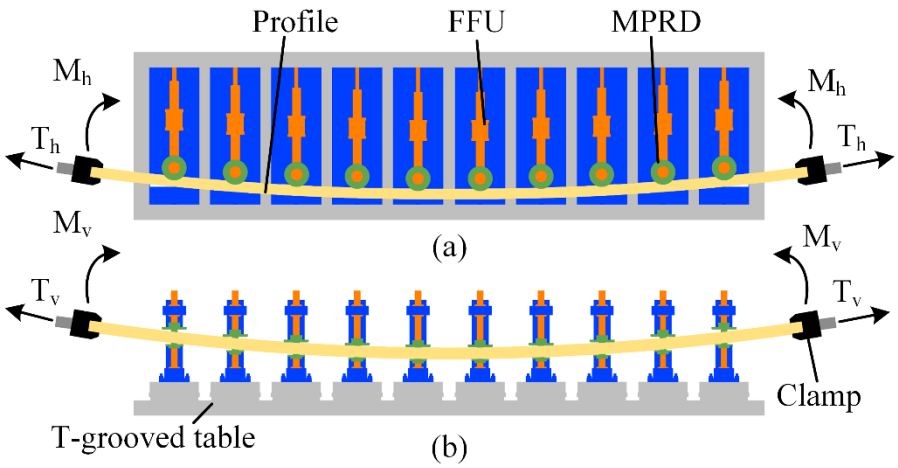

Figure 2. Forming principle of FSB-MPRD. (**a**) Horizontal bending process. (**b**) Vertical bending process.

2.3. Trajectory Design

In order to control the movement track of the clamp accurately, the displacement loading method was adopted in this study. Figure 3 shows the trajectory design of the

clamp and MPRD. In the horizontal bending process, the workpiece was bent in the x–y plane, as shown in Figure 3a.

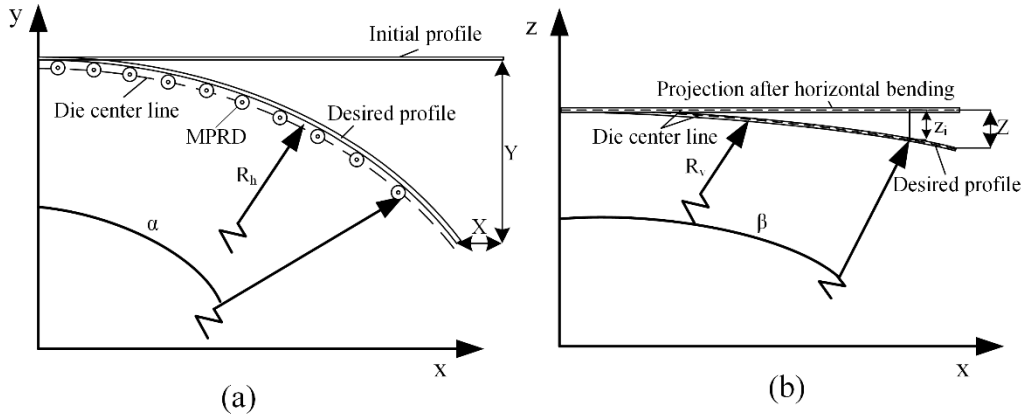

Figure 3. Trajectory design of clamp and MPRD. (**a**) Horizontal bending. (**b**) Vertical bending.

The trajectory of the clamp is given by Equation (2);

$$\begin{cases} X = (L + \delta_{pr}) - \left[(L + \delta_{pr} - \alpha R_h) \cos\alpha + R_h \sin\alpha + d_1 \sin\alpha \right] \\ Y = \left[(L + \delta_{pr} - \alpha R_h) \right] \sin\alpha + R_h(1 - \cos\alpha) + d_1(1 - \cos\alpha) \end{cases} \quad (2)$$

where X and Y are the distances that the clamp moves along the x and y axes, respectively. L is workpiece length, δ_{pr} is the pre-stretching length, R_h is the radius of horizontal bending, α is the angle of horizontal bending, and d_1 a is a constant, representing the distance from the reference point of the clamp to the centroid of the section.

In the vertical bending process, the workpiece was bent in the x–z plane, as shown in Figure 3b. The trajectory of the clamp is given by Equation (3), and the trajectory of the die is given by Equation (6);

$$Z = R_v(1 - \cos\beta) + (L_2 - L_1)\tan\beta \quad (3)$$

$$L_1 = R_h \sin\alpha \quad (4)$$

$$L_2 = R_h \sin\alpha + \left[(L + \delta_{pr}) - \alpha R_h \right] \cos\alpha + d_1 \sin\alpha \quad (5)$$

where Z is the distance that the clamp moves along the z-axis, R_v is the vertical bending radius, and β is the vertical bending angle. L_1 is the projected length of the effective forming zone in the x–z plane, and L_2 is the projected length of the workpiece in the x-z plane.

$$z_j = R_v(1 - \cos\beta_j) \quad (6)$$

$$\beta_j = \arcsin\left(\frac{D_j}{R_v}\right) \quad (7)$$

Among them, z_j is the distance moved by the j-th die along the z-axis, β_j is the bending angle of the workpiece at the j-th die, and D_j is the horizontal distance between the j-th die and the first die.

3. Numerical Simulation

3.1. Finite Element Model

In this study, the Abaqus/Explicit (DASSAULT SIMULIA, Johnston, RI, USA) analysis module was used to simulate the FSB-MPRD forming process. First, we designed the number of MPRD according to the length of the profile. Then, we used Autocad2017 software (Autodesk, CA, USA) to plan the trajectory of the horizontal and vertical bending processes. Finally, the model was established in the ABAQUS software, the shape of the

MPRD was designed, and the steps of assembling, defining interaction, setting material properties, boundary conditions, and meshing were carried out in sequence.

The process parameters of numerical simulation are shown in Table 2. In this study, the Y-profile was selected as the research object. The simplified assembly diagram of the FSB-MPRD forming process is shown in Figure 4a. The model was mainly composed of the Y-profile, clamp, and several MPRD. The contact state between the profile and MPRD was set as general contact, and friction coefficient was set as 0.15. When meshing, the profile has a deformable body, a C3D8R solid element is adopted, the clamp and MPRD are rigid bodies, and the R3D4 rigid body element is adopted. The mesh size of the Y-profile needs to be defined separately. The mesh size was 4 layers thick and 10 mm in length. The mesh element of the clamp and MPRD can be of the default size. The mesh size of the clamp was 10 mm. The mesh size of MPRD was 7 mm.

Table 2. Process parameters of numerical modeling.

Process Parameters	Value
Section shape	Y-profile
Length of profile (mm)	3000
Pre-stretching length δ_{pr} (mm)	30
Post-stretching length δ_{po} (mm)	30.3
Mass scaling factor	300
Friction coefficient	0.15
R_h (mm)	2000, 2500, 3000, 3500
R_v (mm)	6000, 7000, 8000, 9000
Transition zone length (mm)	200, 300, 400, 500
Radius of roller dies R (mm)	50, 55, 60
Wall thickness of profile (mm)	8, 9, 10, 11

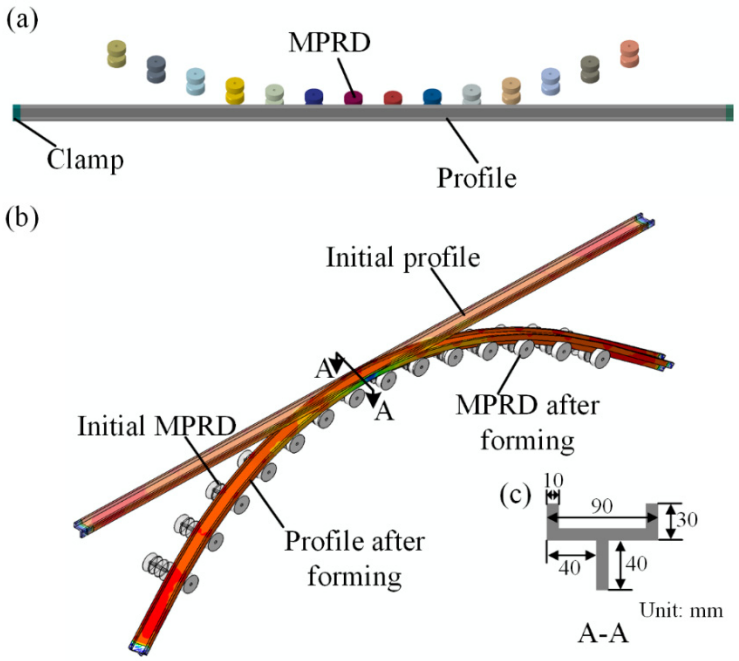

Figure 4. Finite element model. (**a**) Diagram of model assembly. (**b**) Numerical simulation results. (**c**) Cross-section of the Y-profile.

The forming process of FSB-MPRD is mainly divided into four steps: pre-stretching, horizontal bending, vertical bending, and post-stretching. The corresponding simulation time was set as 0.5, 1.5, 1.5, and 0.5, respectively. In order to improve the calculation accuracy of the model, double precision was used for calculation. A simulation test often

takes a long time. In order to improve calculation efficiency, setting a mass scaling factor of 300 can save calculation time on the premise of ensuring calculation accuracy. The numerical simulation result of the Y-profile is shown in Figure 4b. It can be seen from Figure 4b that the Y-profile had undergone 3D deformation, the forming effect was good, and the profile had no obvious surface defects.

3.2. Characterization of Springback

The ABAQUS/Implicit module was used to calculate the springback simulation of the profile after unloading. In order to observe the springback phenomenon of the profile, the original load and boundary conditions were deleted during the springback modeling process, and a fixed constraint was reapplied in the middle of the profile. Due to the three-dimensional deformation of the profile, its springback was more complicated than the traditional two-dimensional stretch bending process, and the evaluation method should be more comprehensive. Therefore, the springback process was divided into horizontal bending springback and vertical bending springback processes. All the nodes of the profile centerline before and after deformation were extracted, and the springback deviation was calculated node by node. The springback deviation was used to characterize the springback change of the profile, as shown in Figure 5a,b.

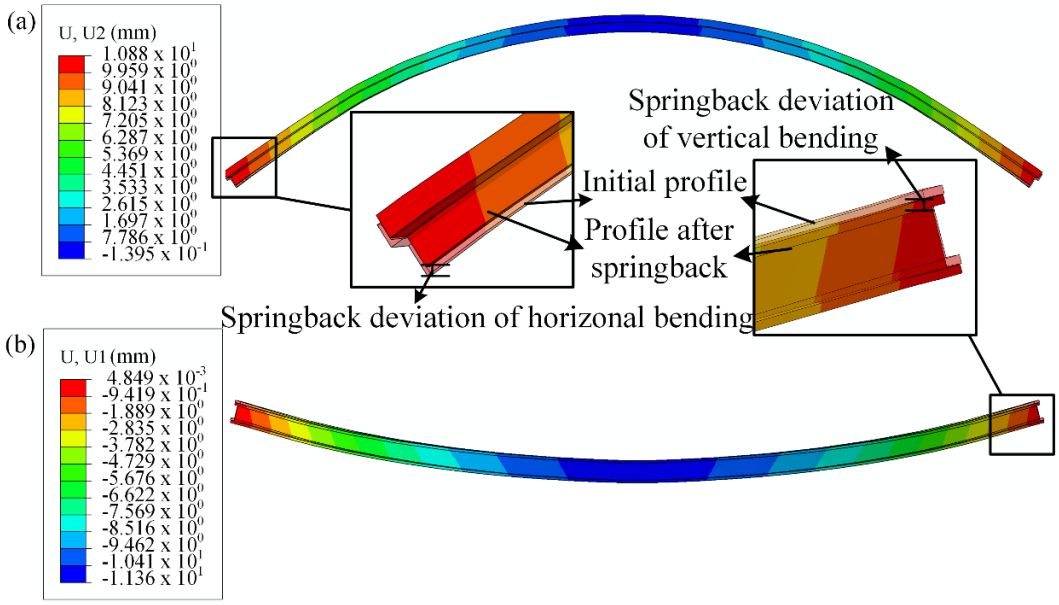

Figure 5. Characterization of springback. (**a**) Definition of springback deviation of horizontal bending. (**b**) Definition of springback deviation of vertical bending.

4. Results and Discussion

4.1. Influence of Horizontal Bending Radius on Springback

When R_v was 7000 mm, transition zone length was 400 mm, R was 50 mm, and wall thickness of the profile was 10 mm; the influence of different horizontal bending radii on springback deviation is studied in the FSB-MPRD process. It can be seen from Figure 6a that when R_h was 3500 mm, the horizontal bending springback deviation of the Y-profile was the minimum. As the horizontal bending target curvature gradually increased, the horizontal bending springback deviation of the Y-profile gradually increased. Compared with the profile with R_h = 3500 mm, the maximum springback deviation of the profile with R_h = 2000 mm in horizontal bending increased by 58.4%. This is mainly due to the increase in the forming radius and the reduction of the deformation degree of the profile, which leads to the reduction of the plastic deformation of the material, thus causing serious

springback. Under the influence of the horizontal bending radius, the springback deviation of vertical bending of the Y-profile also presented the same law. As shown in Figure 6b, with the increase in the horizontal bending radius, the springback deviation of vertical bending of the Y-profile became larger and larger.

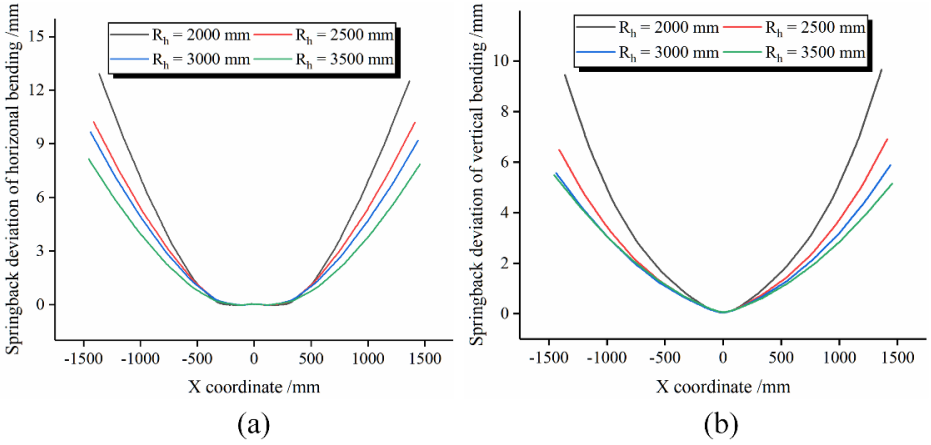

Figure 6. Springback deviation with different horizontal bending radii. (**a**) Springback deviation of horizonal bending. (**b**) Springback deviation of vertical bending.

4.2. Influence of Vertical Bending Radius on Springback

When R_h was 2500 mm, transition zone length was 400 mm, R was 50 mm, and wall thickness of the profile was 10 mm; the influence of different vertical bending radii on the springback deviation is studied. Figure 7a shows the influence of the vertical bending radii on the horizontal bending springback deviation. Although the horizontal bending radii of the profiles in this group of tests were the same, the horizontal bending springback deviation of the Y-profiles was quite different. When the vertical bending target curvature of the profile gradually decreased, the springback of horizontal bending of the Y-profile gradually became more pronounced. Compared with R_v = 9000 mm, the maximum springback deviation of horizontal bending of the R_v = 6000 profile was reduced by 41.9%. Therefore, when the horizontal bending radius was constant, the vertical bending radius of the Y-profile had a great influence on springback deviation of horizontal bending.

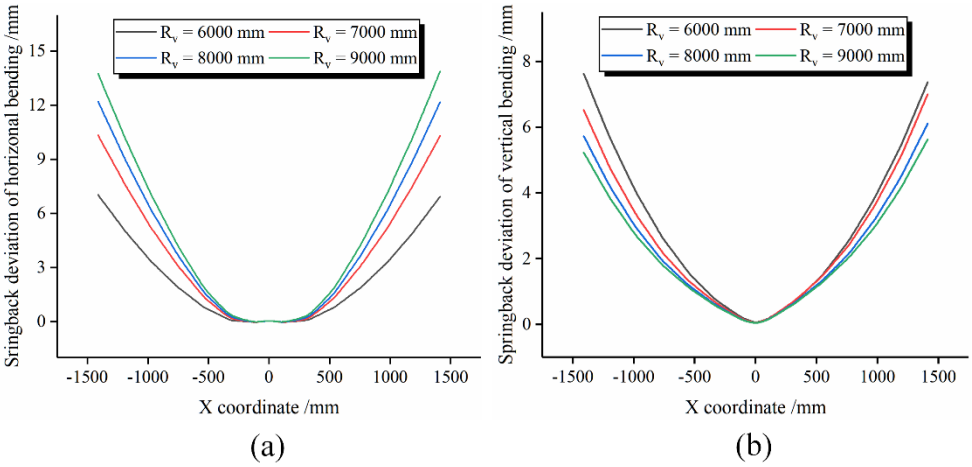

Figure 7. Springback deviation with different vertical bending radii. (**a**) Springback deviation of horizonal bending. (**b**) Springback deviation of vertical bending.

Figure 7b shows that when the horizontal bending radius was constant, the springback deviation of vertical bending decreased with the increase in vertical bending radius. The reasons for this phenomenon are the same as those described in Section 4.1.

4.3. Influence of Transition Zone Length on Springback

The transition zone refers to the section of the profile that exists between the clamping zone and the effective forming zone, and it can also be referred to as the suspended profile section during the forming process. In the forming process of FSB-MPRD, the role of the transition zone is to evenly transfer the force applied by the clamp to the effective forming zone of the profile to ensure the forming quality. In this paper, the profile was divided into the effective forming zone, transition zone, and clamping zone, as shown in Figure 8. In the traditional stretch bending process, the transition zone length is usually set at 100–500 mm. The influence of different transition zone lengths on the springback deviation in the forming process of FSB-MPRD was studied.

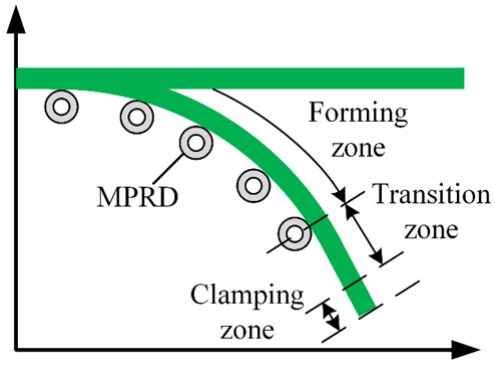

Figure 8. Definition of transition zone length.

Figure 9 shows the influence of different transition zone lengths on springback deviation. In this set of tests, R_h was 2500 mm, R_v was 7000 mm, R was 50 mm, and wall thickness of the profile was 10 mm. It can be seen from Figure 9a,b that when the transition zone length was 200 mm, the springback deviation of horizontal bending and vertical bending of the Y-profile was at a minimum. With the increase in transition zone length, the springback deviation of horizontal bending and vertical bending of the Y-profile increased gradually. Compared with the transition zone length of 200 mm, the maximum springback deviation of the profile with a transition zone length of 500 mm increased by 4.16% in horizontal bending and 15.5% in vertical bending. This is because the longer the transition zone is, the greater the tensile force required and the more uneven the strain distribution. Therefore, the shorter the transition zone length, the smaller the springback deviation of horizontal bending and vertical bending.

4.4. Influence of Radius of Roller Dies on Springback

Figure 10 shows the influence of different radii of roller dies on springback deviation. It can be seen from Figure 10a,b that the springback deviation curves of horizontal bending and vertical bending of profiles processed by a die radius of 50 and 55 mm basically coincided. When the die radius was increased to 60 mm, the springback deviation of horizontal bending and vertical bending increased. This is due to the different radii of the roller dies; the contact point between the die and the profile is different, which affects the deformation uniformity of the profile and leads to the difference of springback deviation. Therefore, the radius of roller dies is one of the important factors that affect the springback deviation in the FSB-MPRD process.

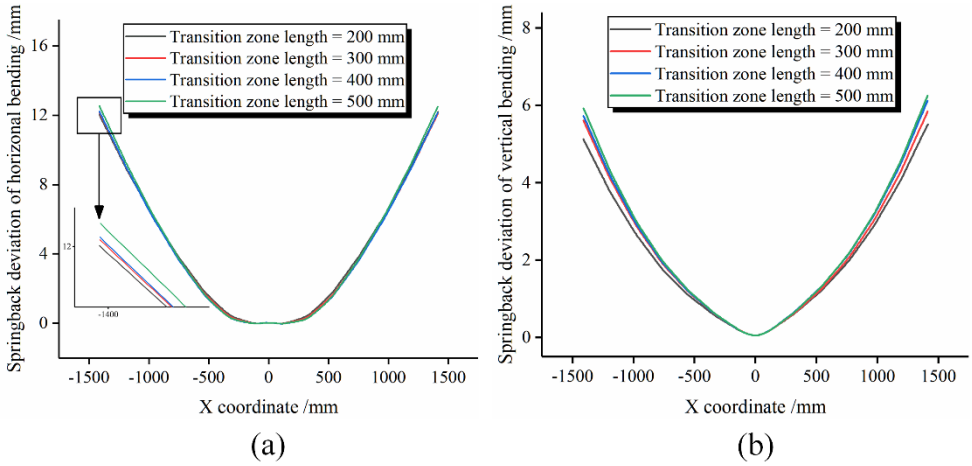

Figure 9. Springback deviation with different transition zone lengths. (**a**) Springback deviation of horizonal bending. (**b**) Springback deviation of vertical bending.

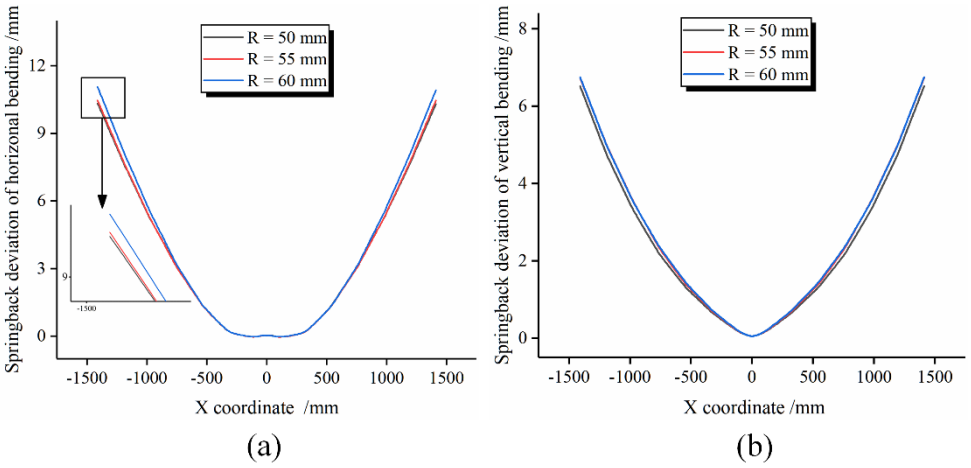

Figure 10. Springback deviation with different radii of roller dies. (**a**) Springback deviation of horizonal bending. (**b**) Springback deviation of vertical bending.

4.5. Influence of Wall Thickness of Profile on Springback

When other process parameters remain unchanged, the influence of a different wall thickness of the profile on the springback deviation can be studied. Figure 11 shows the springback deviation of horizontal bending and vertical bending of the Y-profile with different wall thickness. It can be seen from Figure 11a that although the wall thickness of the profile was different, the springback deviation curves of horizontal bending of the profiles basically coincided. This is mainly because in the horizontal bending process, the target curvature of the profile is large, and the deformation is severe. Therefore, the wall thickness of the profile had little influence on the springback deviation of horizontal bending. However, it can be seen from Figure 11b that in the process of vertical bending, the thinner the wall thickness of the profile, the greater the springback deviation of the profile. This is mainly because the curvature of the target is small in the vertical bending process. If the thickness of the material increases, the relative bending radius of the profile gradually decreases. Therefore, the plastic bending strain increases, the elastic strain decreases, and the springback is reduced.

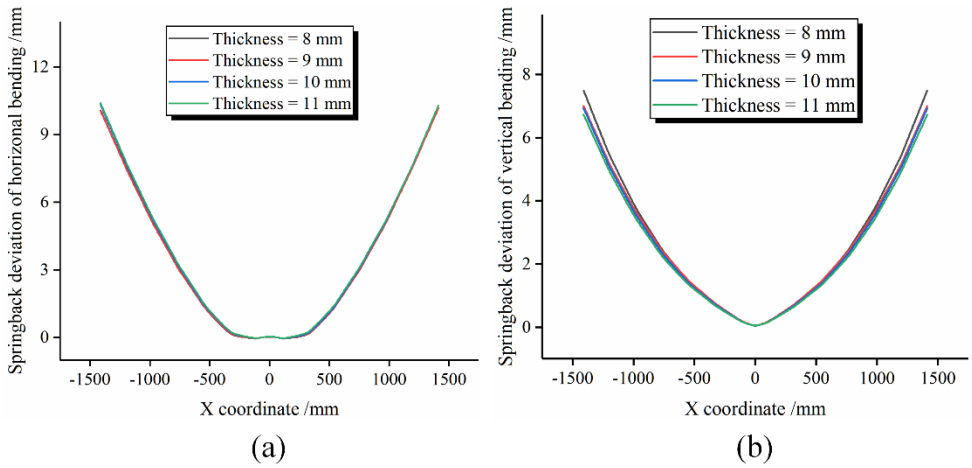

Figure 11. Springback deviation with different wall thickness of the profile. (**a**) Springback deviation of horizonal bending. (**b**) Springback deviation of vertical bending.

5. Experiments

5.1. Experimental Steps

In this paper, experiments were carried out with the FSB-MPRD forming equipment developed by Liang et al [20]. The experimental equipment is shown in Figure 12a. The experimental equipment consisted of 16 flexible foundation units, which can increase or reduce the number of flexible foundation units according to the length of the workpiece. The maximum rotation angle of the manipulator can reach 120° in horizontal bending. The maximum bending angle of the manipulator can reach 60° in vertical bending. Figure 12b shows measuring equipment used to measure the shape error and springback deviation of the profile. Similar to the numerical simulation, the Y-profile was selected as the experimental object. The main process parameters used in the experiment are shown in Table 3.

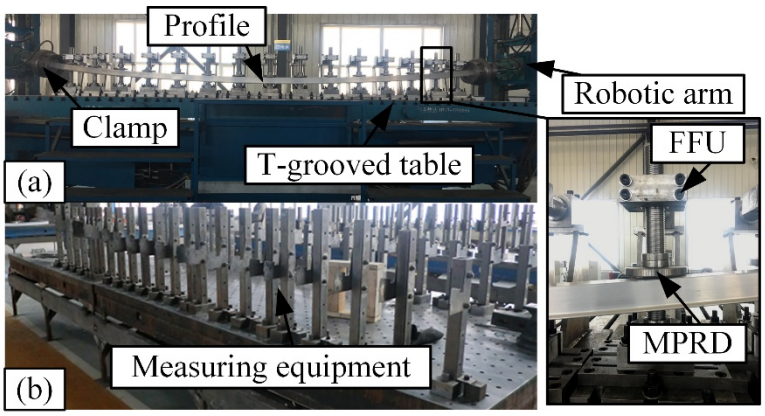

Figure 12. Experimental equipment. (**a**) FSB-MPRD experimental equipment. (**b**) Measuring equipment.

Table 3. Experimental process parameters.

Process Parameters	Value
Section shape	Y-profile
Length of profile (mm)	3000
Pre-stretching length δ_{pr} (mm)	30
Post-stretching length δ_{po} (mm)	30.3
R_h (mm)	2500
R_v (mm)	7000
Transition zone length (mm)	400
Radius of roller dies R (mm)	50

5.2. Experimental Steps

The profile processed by the FSB-MPRD experimental equipment is shown in Figure 13. It can be seen in Figure 13 that the forming quality of the profile was good, its surface had no obvious indentations and wrinkles, and its cross-section had no cross-sectional distortion. Springback measurement equipment is designed according to FSB-MPRD experimental equipment, and its unit body can move freely. The unloaded Y-profile was placed on the springback measurement equipment, and the position of the unit body after springback was recorded and compared with the target shape so as to obtain the springback error.

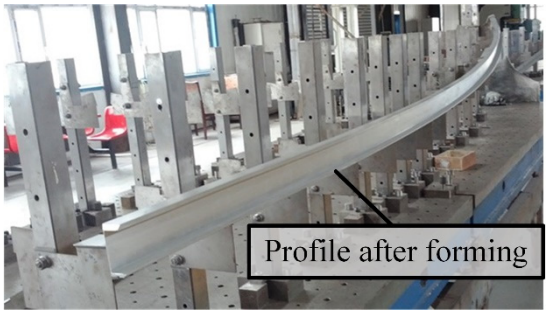

Figure 13. Experimental workpiece.

5.3. Comparison of Springback Deviation

The test data of springback deviation were extracted from the experimental results and compared with the numerical simulation results. The comparison results are shown in Figure 14. It can be seen in Figure 14a,b that the springback deviations of horizontal bending and vertical bending of the Y-profile obtained by numerical simulation and experiment were basically consistent. Additionally, it can be seen in Figure 15 that the maximum springback deviation obtained by experiment as compared to numerical simulation was not much different.

The springback deviation of the Y-profile has been effectively controlled by the combination of the experiment and numerical simulation, and large-scale production has been realized in the enterprise, as shown in Figure 16.

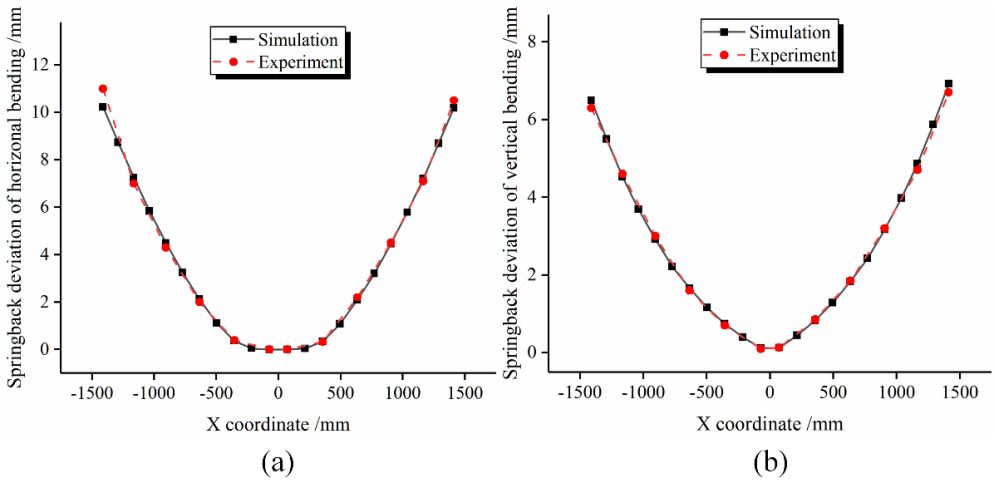

Figure 14. Comparison of springback deviation of Y-profile: (**a**) horizontal bending, (**b**) vertical bending.

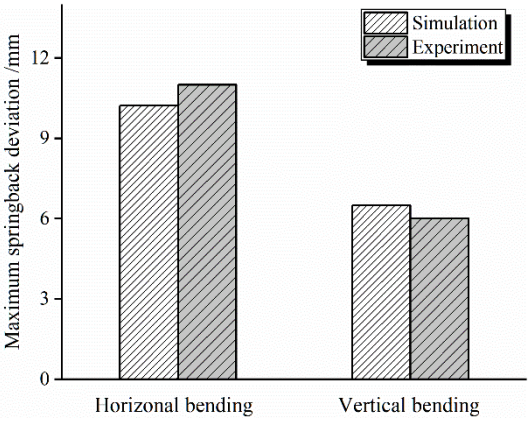

Figure 15. Comparison of maximum springback deviation.

Figure 16. Large-scale production of the Y-profile.

6. Conclusions

In order to grasp the springback law of the profile in the FSB-MPRD process more comprehensively, the influence of process parameters such as horizontal bending radius, vertical bending radius, transition zone length, radius of roller dies, and wall thickness of the profile on springback deviation has been discussed by the numerical simulation method and verified by experiments. The main conclusions are as follows:

1. Horizontal bending radius and vertical bending radius have great influence on springback deviation of the Y-profile. With the increase in horizontal bending radius, the springback deviation of horizontal bending and vertical bending gradually decreases. With the increase in vertical bending radius, the springback deviation of horizontal bending gradually increases, and the springback deviation of vertical bending gradually decreases.
2. The shorter the transition zone length, the smaller the springback deviation of horizontal bending and vertical bending. This is mainly because the longer the transition zone, the greater the tensile force required, and the distribution of stress and strain is more uneven.
3. The smaller the radius of roller dies, the smaller the springback deviation of horizontal bending and vertical bending of the Y-profile. Die radius is also one of the important factors that affect the springback deviation of the workpiece in the FSB-MPRD process.
4. In the horizontal bending process, the wall thickness of the profile has less influence on the springback deviation. However, in the vertical bending process, as the wall thickness increases, the springback deviation gradually decreases.

Author Contributions: C.C. conducted the numerical modeling and wrote the first draft of the manuscript. J.L. provided the concept. Y.L. and C.L. conducted the experiments. W.J. edited the draft of the manuscript. All authors have read and agreed to the published version of the manuscript.

Funding: This research was funded by Project of Jilin Provincial Scientific and Technological Department, grant number 20190302037GX; Project of Jilin Province Development and Reform Commission, grant number 2019C046-2.

Institutional Review Board Statement: Not applicable

Data Availability Statement: The data sets used or analyzed during the current study are available from the corresponding author upon reasonable request.

Acknowledgments: The authors wish to express their gratitude for the support from Jilin Provincial Scientific and Technological Department, and Jilin Provincial Development and Reform Commission.

Conflicts of Interest: The authors declare no conflict of interest.

References

1. Leu, D.-K.; Zhuang, Z.-W. Springback prediction of the vee bending process for high-strength steel sheets. *J. Mech. Sci. Technol.* **2016**, *30*, 1077–1084. [CrossRef]
2. Zhang, S.; Wu, J. Springback prediction of three-dimensional variable curvature tube bending. *Adv. Mech. Eng.* **2016**, *8*, 168781401663732. [CrossRef]
3. Nikhare, C.P. Springback Reduction by Using Tool Rollers. *Int. J. Precis. Eng. Manuf.* **2019**, *21*, 67–74. [CrossRef]
4. Zhang, Z.; Wu, J.; Guo, R.; Wang, M.; Li, F.; Guo, S.; Wang, Y.; Liu, W. A semi-analytical method for the springback prediction of thick-walled 3D tubes. *Mater. Des.* **2016**, *99*, 57–67. [CrossRef]
5. Wu, J.; Zhang, Z.; Shang, Q.; Li, F.; Wang, Y.; Hui, Y.; Fan, H. A method for investigating the springback behavior of 3D tubes. *Int. J. Mech. Sci.* **2017**, *131–132*, 191–204. [CrossRef]
6. Zhang, D.; Li, Y.; Liu, J.; Xie, G.; Su, E. A novel 3D optical method for measuring and evaluating springback in sheet metal forming process. *Measurement* **2016**, *92*, 303–317. [CrossRef]
7. Ouakdi, E.; Louahdi, R.; Khirani, D.; Tabourot, L. Evaluation of springback under the effect of holding force and die radius in a stretch bending test. *Mater. Des.* **2012**, *35*, 106–112. [CrossRef]
8. Wasif, M.; Iqbal, S.A.; Tufail, M.; Karim, H. Experimental Analysis and Prediction of Springback in V-bending Process of High-Tensile Strength Steels. *Trans. Indian Inst. Met.* **2019**, *73*, 285–300. [CrossRef]
9. Zhan, M.; Wang, Y.; Yang, H.; Long, H. An analytic model for tube bending springback considering different parameter variations of Ti-alloy tubes. *J. Mater. Process. Technol.* **2016**, *236*, 123–137. [CrossRef]

10. Vasudevan, D.; Srinivasan, R.; Padmanabhan, P. Effect of process parameters on springback behaviour during air bending of electrogalvanised steel sheet. *J. Zhejiang Univ. A* **2011**, *12*, 183–189. [CrossRef]
11. Chen, M.E.D. Numerical Solution of Thin-walled Tube Bending Springback with Exponential Hardening Law. *Steel Res. Int.* **2010**, *81*, 286–291. [CrossRef]
12. Liu, Y.E.D. Springback and time-dependent springback of 1Cr18Ni9Ti stainless steel tubes under bending. *Mater. Des.* **2010**, *31*, 1256–1261. [CrossRef]
13. Farhadi, A.; Nayebi, A. Springback analysis of thick-walled tubes under combined bending-torsion loading with consideration of nonlinear kinematic hardening. *Prod. Eng.* **2020**, *14*, 135–145. [CrossRef]
14. Ozturk, F.; Toros, S.; Kilic, S.; Bas, M.H. Effects of cold and warm temperatures on springback of aluminium—Magnesium alloy 5083-H111. *Proc. Inst. Mech. Eng. Part. B J. Eng. Manuf.* **2009**, *223*, 427–431. [CrossRef]
15. Rahmani, B.; Alinejad, G.; Bakhshi-Jooybari, M.; Gorji, A. An investigation on springback/negative springback phenomena using finite element method and experimental approach. *Proc. Inst. Mech. Eng. Part. B J. Eng. Manuf.* **2009**, *223*, 841–850. [CrossRef]
16. Li, L.; Seo, Y.-H.; Heo, S.-C.; Kang, B.-S.; Kim, J. Numerical simulations on reducing the unloading springback with multi-step multi-point forming technology. *Int. J. Adv. Manuf. Technol.* **2009**, *48*, 45–61. [CrossRef]
17. Abebe, M.; Yoon, J.-S.; Kang, B.-S. Radial Basis Functional Model of Multi-Point Dieless Forming Process for Springback Reduction and Compensation. *Metals* **2017**, *7*, 528. [CrossRef]
18. Wang, A.; Zhong, K.; El Fakir, O.; Liu, J.; Sun, C.; Wang, L.-L.; Lin, J.; Dean, T.A. Springback analysis of AA5754 after hot stamping: Experiments and FE modelling. *Int. J. Adv. Manuf. Technol.* **2016**, *89*, 1339–1352. [CrossRef]
19. Liu, Z.; Li, L.; Wang, G.; Chen, J.; Yi, J. Springback behaviors of extruded 6063 aluminum profile in subsequent multi-stage manufacturing processes. *Int. J. Adv. Manuf. Technol.* **2020**, *109*, 1–13. [CrossRef]
20. Liang, J.; Chen, C.; Li, Y.; Liang, C. Effect of roller dies on springback law of profile for flexible 3D multi-point stretch bending. *Int. J. Adv. Manuf. Technol.* **2020**, *108*, 3765–3777. [CrossRef]